

Band-Gap Guidance in Optically Induced Photonic Lattices with a Negative Defect

Igor Makasyuk¹ and Zhigang Chen^{1,2}

¹*Department of Physics and Astronomy, San Francisco State University, San Francisco, California 94132, USA*

²*TEDA Applied Physical School, Nankai University, Tianjin 300457, China*

Jianke Yang

*Department of Mathematics and Statistics, University of Vermont, Burlington, Vermont 05401, USA,
and Zhou Pei-Yuan Center for Applied Mathematics, Tsinghua University, Beijing, China*

(Received 8 December 2005; published 6 June 2006)

We report the first experimental demonstration of band-gap guidance of light in an optically induced two-dimensional photonic lattice with a single-site negative defect (akin to a low-index core in photonic-crystal fibers). We discuss the difference between spatial guidance at a regular and a defect site, and show that the guided beam through the defect displays fine structures such as vortex cells that arise from defect modes excited at higher band gaps. Defect modes at different wavelengths are also observed.

DOI: [10.1103/PhysRevLett.96.223903](https://doi.org/10.1103/PhysRevLett.96.223903)

PACS numbers: 42.70.Qs, 42.65.Tg

Light propagation in photonic crystals or periodic photonic structures in general is of great interest to both fundamental physics and applications [1–4]. In uniformly periodic waveguide lattices such as those fabricated in nonlinear materials and those optically induced in photorefractive crystals, experiments have demonstrated a number of novel phenomena of light propagation including discrete solitons, discrete vortices, Floquet-Bloch solitons, Bloch oscillations, and Zener tunneling [5–9]. On the other hand, periodic lattices with impurities and defects are well known in solid state physics, photonic crystals [1,2], and fabricated semiconductor waveguide arrays [10]. In particular, band-gap guidance (BG) by defects in otherwise uniformly periodic structures such as hollow-core photonic-crystal fibers (PCFs) is fundamentally different from traditional guidance by total internal reflection (TIR) [1,2]. Such BGs have been demonstrated earlier in two-dimensional (2D) arrays of dielectric cylinders with isolated defects for microwaves [11], and recently in all-solid PCFs with a lower-index core for optical waves [12]. In fact, BG has been studied for a wide range of spectra, and laser emission based on photonic defect modes (DMs) has been realized in a number of experiments [13].

In photonic lattices optically induced in a photorefractive crystal [7–9,14], the induced refractive index variation is typically orders of magnitude smaller than that in photonic crystals, while the lattice spacing is also much larger than the optical wavelength. A natural question arises: is it possible to optically induce 2D waveguide lattices with a single-site defect so that light can be confined in the defect akin to those achieved in hollow-core PCFs? That would open up another avenue in studying the defect-related phenomena in periodic systems, taking advantage of the unusual features of photorefractive materials such as wavelength-sensitive and reconfigurable nonlinear refractive index patterns induced at very low power levels.

In photonic crystals and PCFs, it is prevalent to analyze the propagation of light using band-gap diagrams (also

called “finger diagrams”). Such diagrams show the ranges of frequency modes as a function of wave vectors where the propagation constant is either real (propagation allowed—Bloch bands) or imaginary (propagation forbidden—band gaps). Within the gaps, frequency modes cannot exist but light can be localized by defects that support evanescent defect states or DMs [1,2]. In waveguide lattices, often the analysis of how a monochromatic light field distributes itself focuses on the band-gap diagrams of spatial frequency modes (propagation constant vs transverse wave vector) [6,9,15]. Although recent work has revealed the existence of DMs in 1D waveguide lattices [6,10,16], experimental demonstration of BG by defects in 2D photonic lattices has remained a challenge.

In this Letter, we report the first experimental demonstration of BG in optically induced 2D photonic lattices with a single-site negative defect. In such a defect, the refractive index has its minimum as compared to that in the surrounding “rods” (akin to an “air defect” in photonic crystals or hollow-core PCFs [1,2], and much like all-solid low-index-core PCFs [12]). We observe that a probe beam at different wavelengths is spatially confined in the defect during its linear propagation, although the defect is repulsive and the beam itself has no nonlinear self-action. The observed “guidance” of light in the negative defect arises from linear propagation of the DM formed in the spatial band gap of the photonic lattice, which is fundamentally different from linear guidance by TIR or nonlinear self-guidance as in a spatial soliton. In addition, we show that the “guided” patterns by the defect display fine spatial structures such as dipole and vortex cells which arise from the DM excited at higher band gaps. To our knowledge, a higher band DM has not been observed before in any system. Our optical induction of reconfigurable photonic lattices with defects not only has a direct link to technologically important systems of periodic structures such as PCFs, but also brings about the possibility for studying, in an optical setting, many novel phenomena in periodic

systems beyond optics such as defect healing, eigenmode splitting, and nonlinear mode coupling which have been intriguing scientists for decades.

The experimental setup used for this study is similar to that used in previous work on soliton lattices [14] and discrete solitons [8], except that we now introduce a defect into an otherwise uniform lattice. The lattice is induced in a photorefractive SBN (strontium barium niobate) crystal by a spatially modulated partially coherent light beam ($\lambda = 488$ nm) sent through a specially designed amplitude mask. The mask is appropriately imaged onto the input face of the crystal, creating a periodic input intensity pattern with a single defect as shown in Fig. 1(a). Such a defect typically fades away quickly during linear propagation [Fig. 1(b)], even if the Talbot self-imaging is suppressed by adjusting the spatial coherence and the Fourier spectrum of the lattice beam. In order to maintain the defect, we “fine-tune” the level of the nonlinearity experienced by the lattice beam, which is controlled by the bias field across the crystal as well as the lattice beam intensity and polarization. In particular, we introduce a small extraordinary component of polarization in the lattice beam ($\sim 20\%$), since with a fully ordinarily polarized beam we can maintain the lattice (as used in previous lattice-soliton experiments [7,8]) but not the defect. The addition of an extraordinary component in the lattice beam leads to a deeper refractive index modulation, taking advantage of the anisotropic property of the photorefractive crystal [8]. In essence, with the help of “adjustable” nonlinearity, a nearly invariant 2D waveguide lattice is induced while maintaining the defect during propagation throughout a 20-mm-long crystal [Fig. 1(c)]. For probing through the defect, we launch a coherent Gaussian beam (wavelength can be varied) into the defect site and have it propagate collinearly with the lattice beam. The probe beam is extraordinarily polarized so it “feels” the periodic

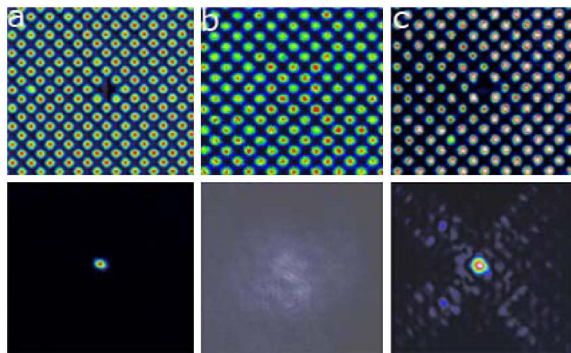


FIG. 1 (color online). Top panel: Intensity pattern of a 2D induced lattice with a single-site negative defect at crystal input (a) and output (b),(c). The defect disappears in the linear regime (b) but can survive with weak nonlinearity (c) after propagating through a 20-mm-long crystal. Bottom panel: Input (a) and output (b),(c) of a probe beam showing band-gap guidance by the defect (c) and normal diffraction without the lattice (b) under the same bias condition.

index variation as induced by the lattice beam, but it does not have appreciable nonlinear self-action itself either by setting its intensity to be weak enough (when at 488 nm) or choosing its wavelength to be much less photosensitive for our SBN crystal.

Typical experimental results on 2D defect modes are presented in the bottom panel of Fig. 1, where Fig. 1(a) is the input intensity pattern of the probe beam ($\lambda = 488$ nm), and Figs. 1(b) and 1(c) show the corresponding patterns after propagating through the crystal. When launched into the defect channel, the Gaussian-like beam evolves into a DM, with most of its energy concentrated in the defect site while the tails along the principal axes of the square lattice (which are diagonally oriented) are clearly visible [Fig. 1(c)]. On the other hand, should the defective lattice be removed, the probe beam alone shows no nonlinear self-action [Fig. 1(b)] under the same bias condition. For this experiment, the lattice spacing (“pitch,” or center-to-center spacing between the index rods) is $\Lambda = 27$ μm , the bias field is $E = 2.8$ kV/cm, and the intensity ratio of the lattice to the probe beam is 3 to 1. A fundamental feature of the BG established in all our observations is that the DMs have long “tails” in the directions of the lattice principal axes [as shown in Fig. 1(c)], in contrast to the 2D discrete diffraction in a uniform lattice where tails are along the diagonal directions of the lattice axes [8].

A series of experiments has been performed to show the fundamental difference between BG and conventional TIR guidance. This difference reflects both in the near-field intensity pattern and power spectrum in Fourier space. In the same 2D photonic lattice ($\Lambda = 27$ μm) as shown in Fig. 1, the probe beam of the same wavelength (488 nm) is launched into a regular lattice site and a defect site under the same experimental conditions for comparison. Figure 2 (top panel) shows such comparison where both the near-field patterns and Fourier spectra are displayed for the DM [Figs. 2(a) and 2(b)] and the TIR guided beam [Figs. 2(c) and 2(d)]. For the DM, the directions of the long tails are along the principal axes of the 2D square lattice, and the corresponding Fourier spectrum illustrates the first Brillouin zone of the lattice where the location of high

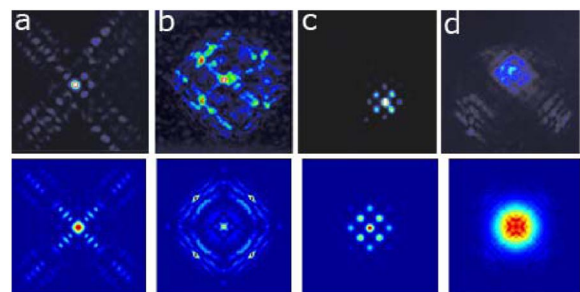


FIG. 2 (color online). Output intensity patterns (a),(c) and Fourier spectra (b),(d) for band-gap guidance at a defect site (a),(b) vs TIR guidance at an off-center regular lattice site (c),(d). Top panel: Experimental results. Bottom panel: Corresponding numerical results.

symmetry points is clearly visible [2,17]. For the TIR guidance at a regular lattice site, the probe beam is well confined around that site, and its power spectrum shows no characteristic spatial frequency. In fact, by increasing or decreasing the lattice potential (thus changing the effective coupling length), the probe can be confined into a single lattice site or coupled into many lattice sites along the diagonal directions as in 2D discrete diffraction [8], in which both its intensity pattern and power spectrum are in distinction with that of the DM. Our observations are corroborated by numerical simulations based on a 2D continuum model with a negative defect in the periodic lattice potential $iU_z + U_{xx} + U_{yy} - \frac{E_0}{1+I_L(x,y)}U = 0$, where U is the envelope function of the beam, E_0 is the applied voltage, and $I_L(x,y) = I_0 \sin^2(\frac{x+y}{\sqrt{2}}) \sin^2(\frac{x-y}{\sqrt{2}}) [1 - \varepsilon \exp(-\frac{(x^2+y^2)^4}{128})]$ is the transverse intensity function of the lattice with a defect (I_0 is the lattice peak intensity, and ε the defect depth) [16]. The corresponding numerical results for $I_0 = 3$ and $\varepsilon = 1$ are illustrated in the bottom panel of Fig. 2. The DMs are well confined in space, and their field distributions do not change over propagation distance.

Using the same probing wavelength ($\lambda = 488$ nm), we observed the formation of DMs at different lattice conditions. One of the intriguing phenomena is the fine structures observed in the long tails of the DM patterns. In Fig. 3, three such characteristic patterns are presented. At $\Lambda = 27$ μm , the tails resulting from the leakage of light extend afar from the center core and cover more than just a single diagonal line of the lattice [Figs. 2(a) and 3(a)]. At $\Lambda = 42$ μm , the tails in the output patterns display even more interesting fine structures associated with nontrivial phase distribution [Figs. 3(b) and 3(c)]. Such a phase pattern was recorded by the interference between the probe beam forming the DM and a broad beam (quasiplane wave). It revealed that the tails along the lattice principal axes contain either dipolelike [Fig. 3(b)] or vortexlike [Fig. 3(c)] arrays. Figure 3(d) shows a typical interferogram corresponding to the intensity pattern of Fig. 3(c), where the locations of vortices are indicated by arrows. It is apparent that the vortex cells have a different sign of topological charge in the two diagonal tails.

These fine structures of the DM can be explained by superposition of DMs at higher band gaps using the above

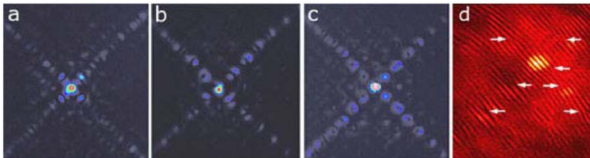


FIG. 3 (color online). Intensity patterns of the DM under different lattice conditions. (a) Lattice spacing $\Lambda = 27$ μm , bias field $E = 2.6$ kV/cm; (b) $\Lambda = 42$ μm , $E = 2.4$ kV/cm; (c) $\Lambda = 42$ μm , $E = 3.0$ kV/cm. (d) Zoom-in interferogram of (c) with a plane wave where arrows indicate location of vortices. The brightest spot corresponds to the defect site.

2D model. The band-gap structure for a 2D uniform lattice is plotted in Fig. 4(a), where μ is the propagation constant. We have obtained DMs in various band gaps for a wide range of physical parameters. In some cases, two independent DMs coexist. Their linear superposition can lead to different phase and intensity patterns. A typical example corresponding to point D in Fig. 4(a) is shown in Figs. 4(b) and 4(c), which was obtained at $I_0 = 3$ and $\varepsilon = 0.1$. Point D lies in the higher band-gap between the second and third Bloch bands (but very close to the right edge of the second band). Figure 4(b) illustrates a DM solution $\psi(x,y)$ found at point D which has dipole-type structures. Another linearly independent DM at point D is $\psi(y,x)$. When these two DMs are combined as $\psi(x,y) + i\psi(y,x)$ with a locked phase delay of $\pi/2$, a new DM possessing a vortex-array structure is obtained [Fig. 4(c)]. These vortices are located inside individual lattice sites with opposite charges between adjacent sites. The similarity between Figs. 4(c), 3(c), and 3(d) indicates that the DM structure observed in Fig. 3(c) arises from the superposition of DMs at higher band gaps. We did a similar analysis of DMs in lower band gaps (below the second Bloch band) in Fig. 4(a) and found that the vortex arrays shown in Fig. 4(c) cannot form at lower band gaps. We note that the DM observed here is somewhat related to the second-band vortex solitons in 2D lattices [17]. We also note that the formation of vortex arrays as a superposition of DMs is analogous to generation of a single vortex by superposition of two phase-locked transverse modes in a laser [18].

In order to find optimal conditions for BG so that light can be well confined by the defect, we performed a series of experiments at different lattice conditions (lattice spacing, intensity, and polarization) and different probe wavelengths. The depth and spacing of the lattice potential is one of the major parameters determining the band gaps in the photorefractive lattice as controlled by the lattice conditions. For instance, we could not observe BG by defect if the lattice spacing is too large ($\Lambda > 50$ μm). The purpose of probing at different wavelengths is twofold: First, a much less photosensitive wavelength ($\lambda = 633$ nm or larger) is used to exclude any possibility of self-action of

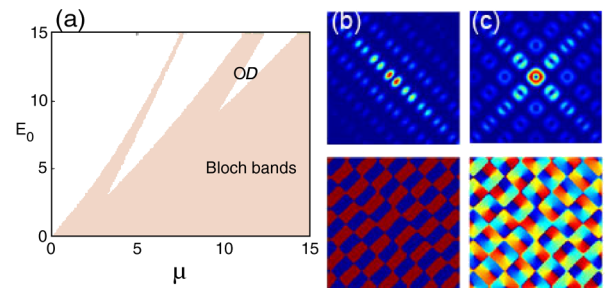


FIG. 4 (color online). (a) Band-gap structure of a 2D uniform lattice ($I_0 = 3$); (b) a defect mode $\psi(x,y)$ found at point D in (a) with $\varepsilon = 0.1$; (c) a linear superposition of defect modes $\psi(x,y)$ and $\psi(y,x)$ with a $\pi/2$ -phase delay. (b),(c) Upper panel shows intensity patterns and lower panel the phase plots.

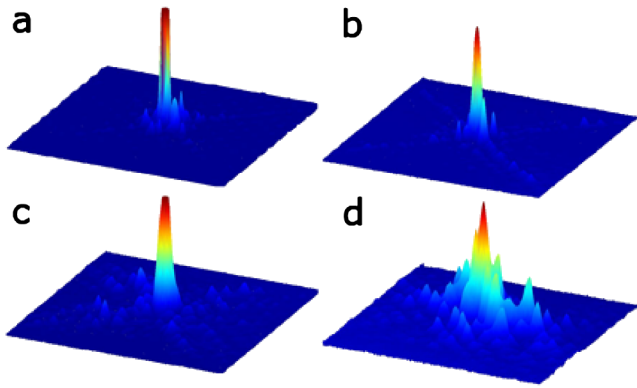


FIG. 5 (color online). Band-gap guidance of a probe beam at different wavelengths: (a) 455 nm, (b) 488 nm, (c) 633 nm, and (d) 785 nm. $\Lambda = 27 \mu\text{m}$ and $E = 2.4 \text{ kV/cm}$.

the probe beam. Second, other wavelengths are used to test the sensibility of the DM to wavelength. Figure 5 shows our experimental results, where four different wavelengths available are employed to test the BG under the same lattice conditions. As seen from Fig. 5, better confinement of light by defect is realized at shorter wavelengths [Figs. 5(a) and 5(b)]. As the wavelength increases to 785 nm within our experimental capability, the confinement deteriorates and the probe beam covers many lattice sites beyond the defect [Fig. 5(d)]. We mention that the frequency dependence of BG has been studied lately with all-solid PCFs [12], where parameters close to what we have in optically induced lattices have been used (e.g., low refractive index contrast of 10^{-2} , large pitch up to $15 \mu\text{m}$), as opposed to the high-index contrast and small pitch typically expected for photonic-crystal structures. It has been shown that those all-solid PCFs are capable of confining light to a single-site negative defect with a transmission spectrum spanning from 700 to 1200 nm.

Several issues merit discussion. To demonstrate clearly that the confinement of light is due to BG rather than TIR guidance by the waveguide lattice, it is essential to monitor both the lattice and the probe beam at input/output faces of the crystal. In all our experiments, we observed that the DM has its peak centered in the negative-defect site where guidance by conventional TIR is prevented. In that regard, DMs in negative defects are far more interesting than those in positive defects, as the latter can support guidance by TIR [16]. An obvious way to create a positive (negative) defect experimentally is to launch an additional narrow beam into a single lattice site with a positive (negative) bias field, as this additional beam increases (decreases) the index of refraction in the targeted lattice site. We found that such a method, although experimentally convenient, is not effective for creating a single-site defect necessary for the observation of BG, simply because the narrow beam diffracts dramatically but the lattice beam does not. With a wide beam (covering several lattice sites) superimposed on the lattice, one could obtain only a far-field visualization of the DM [17]. Our way of inducing a single-site negative

defect enables the observation of strongly localized states with a bright spot in the central regions of both near-field and far-field patterns [Figs. 2(a) and 2(b)].

In summary, we have optically “fabricated” 2D photonic lattices with a single-site negative defect and demonstrated BG at different wavelengths in such reconfigurable lattices. We have observed and explained theoretically the DM excited at higher band gaps. Our work may prove to be relevant to studies of similar phenomena in other periodic systems beyond optics including, for example, matter waves in Bose-Einstein condensates trapped in 2D optical lattices [19] and water waves in periodic cylinder arrays [20].

This work was supported by NSF, AFOSR, PRF, NSFC, and NASA EPSCoR grants. We thank S. Fan, D. Skryabin, D. Neshev, J. Young, and X. Wang for assistance.

-
- [1] P. St. J. Russell, *Science* **299**, 358 (2003).
 - [2] J. D. Joannopoulos *et al.*, *Photonic Crystals: Molding the Flow of Light* (Princeton University Press, Princeton, NJ, 1995).
 - [3] D. N. Christodoulides, F. Lederer, and Y. Silberberg, *Nature (London)* **424**, 817 (2003); D. N. Christodoulides and R. I. Joseph, *Opt. Lett.* **13**, 794 (1988).
 - [4] Y. S. Kivshar and G. P. Agrawal, *Optical Solitons: From Fibers to Photonic Crystals* (Academic Press, New York, 2003).
 - [5] H. S. Eisenberg *et al.*, *Phys. Rev. Lett.* **81**, 3383 (1998).
 - [6] D. Mandelik *et al.*, *Phys. Rev. Lett.* **90**, 053902 (2003); A. Sukhorukov *et al.*, *ibid.* **92**, 093901 (2004).
 - [7] J. W. Fleischer *et al.*, *Nature (London)* **422**, 147 (2003); D. Neshev *et al.*, *Opt. Lett.* **28**, 710 (2003).
 - [8] H. Martin *et al.*, *Phys. Rev. Lett.* **92**, 123902 (2004); D. N. Neshev *et al.*, *ibid.* **92**, 123903 (2004); J. W. Fleischer *et al.*, *ibid.* **92**, 123904 (2004); Z. Chen *et al.*, *ibid.* **92**, 143902 (2004); J. Yang *et al.*, *ibid.* **94**, 113902 (2005).
 - [9] H. Trompeter, *Phys. Rev. Lett.* **96**, 053903 (2006).
 - [10] U. Peschel *et al.*, *Appl. Phys. Lett.* **75**, 1348 (1999); R. Morandotti *et al.*, *Opt. Lett.* **28**, 834 (2003).
 - [11] S. L. McCall *et al.*, *Phys. Rev. Lett.* **67**, 2017 (1991); E. Yablonovitch *et al.*, *ibid.* **67**, 3380 (1991); M. Bayindir *et al.*, *ibid.* **84**, 2140 (2000).
 - [12] F. Luan *et al.*, *Opt. Lett.* **29**, 2369 (2004); A. Argyros *et al.*, *Opt. Express* **13**, 309 (2005).
 - [13] J. S. Foresi *et al.*, *Nature (London)* **390**, 143 (1997); S. Fan *et al.*, *Phys. Rev. Lett.* **80**, 960 (1998); O. Painter *et al.*, *Science* **284**, 1819 (1999); J. Schmidtke *et al.*, *Phys. Rev. Lett.* **90**, 083902 (2003); X. Wu *et al.*, *Appl. Phys. Lett.* **85**, 3657 (2004).
 - [14] Z. Chen and K. McCarthy, *Opt. Lett.* **27**, 2019 (2002).
 - [15] N. K. Efremidis *et al.*, *Phys. Rev. Lett.* **91**, 213906 (2003).
 - [16] F. Fedele *et al.*, *Opt. Lett.* **30**, 1506 (2005); *Stud. Appl. Math.* **115**, 279 (2005).
 - [17] G. Bartal *et al.*, *Phys. Rev. Lett.* **94**, 163902 (2005); **95**, 053904 (2005).
 - [18] C. Tamm and C. O. Weiss, *J. Opt. Soc. Am. B* **7**, 1034 (1990).
 - [19] B. Eiermann, *Phys. Rev. Lett.* **92**, 230401 (2004).
 - [20] X. Hu *et al.*, *Phys. Rev. Lett.* **95**, 154501 (2005).